JOURNAL OF THE ROYAL SOCIETY Interface

Rapid magnetic cell delivery for large tubular bioengineered constructs

J. Gonzalez-Molina, J. Riegler, P. Southern, D. Ortega, C. C. Frangos, Y. Angelopoulos, S. Husain, M. F. Lythgoe, Q. A. Pankhurst and R. M. Day

J. R. Soc. Interface published online 13 June 2012
doi: 10.1098/rsif.2012.0316

JOURNAL OF THE ROYAL SOCIETY Interface

FirstCite® e-publishing

J. R. Soc. Interface
doi:10.1098/rsif.2012.0316
Published online

Rapid magnetic cell delivery for large tubular bioengineered constructs

J. Gonzalez-Molina[1], J. Riegler[2], P. Southern[3,4], D. Ortega[3,4], C. C. Frangos[1], Y. Angelopoulos[1], S. Husain[1], M. F. Lythgoe[2], Q. A. Pankhurst[3,4] and R. M. Day[1,*]

[1]*Biomedical Engineering Group, Centre for Gastroenterology and Nutrition, Division of Medicine, and* [2]*Centre for Advanced Biomedical Imaging (CABI), Division of Medicine and Institute of Child 5 Health, Centre for Mathematics and Physics in the Life Sciences and Experimental Biology (CoMPLEX), University College London (UCL), London WC1E 6DD, UK*
[3]*Davy-Faraday Research Laboratory, The Royal Institution of Great Britain, 21 Albemarle Street, London W1S 4BS, UK*
[4]*Department of Physics and Astronomy, University College London, London WC1E 6BT, UK*

Delivery of cells into tubular tissue constructs with large diameters poses significant spatial and temporal challenges. This study describes preliminary findings for a novel process for rapid and uniform seeding of cells onto the luminal surface of large tubular constructs. Fibroblasts, tagged with superparamagnetic iron oxide nanoparticles (SPION), were directed onto the luminal surface of tubular constructs by a magnetic field generated by a k4-type Halbach cylinder device. The spatial distribution of attached cells, as measured by the mean number of cells, was compared with a conventional, dynamic, rotational cell-delivery technique. Cell loading onto the constructs was measured by microscopy and magnetic resonance imaging. The different seeding techniques employed had a significant effect on the spatial distribution of the cells ($p < 0.0001$). The number of attached cells at defined positions within the same construct was significantly different for the dynamic rotation technique ($p < 0.05$). In contrast, no significant differences in the number of cells attached to the luminal surface were found between the defined positions on the construct loaded with the Halbach cylinder. The technique described overcomes limitations associated with existing cell-delivery techniques and is amenable to a variety of tubular organs where rapid loading and uniform distribution of cells for therapeutic applications are required.

Keywords: Halbach array; cell therapy; tissue engineering; gastroenterology

1. INTRODUCTION

The number of people requiring organ transplantation continues to outnumber the quantity of suitable donor organs available. To address these shortages, artificial replacement of hollow organs (such as those of the circulatory, respiratory, gastrointestinal and genitourinary systems) has been sought for many years. Recent advancements in regenerative medicine have demonstrated the feasibility of tissue engineering of hollow organs for transplantation into humans. Tissue engineering of hollow organs typically involves the delivery of cells onto a biocompatible three-dimensional structure that is designed to function as a scaffold that will enable cell attachment and guidance of cells into a tissue construct with the desired configuration. The most numerous examples of tissue-engineered tubular constructs are related to the circulatory system [1] (e.g. vascular grafts), but, more recently, other tissue-engineered hollow organs have been successfully transplanted into humans, including respiratory [2] and genitourinary [3] tissues. While these pioneering studies represent major advances in human healthcare, there remains scope for significant improvement in the various processes underlying these technologies before they can be considered optimized, reproducible and ready for widespread use.

The rapid and efficient loading of cells onto large tubular tissue engineering scaffolds is one process that especially needs further attention. Often, only limited quantities of donor or autologous cells are available for seeding onto a tissue-engineered construct. There is therefore a need to deliver cells in an efficient manner, in terms of both speed of process (to maintain cellular viability) and the number of cells (to avoid wastage). Moreover, the distribution of cells should be uniform to ensure that confluent coverage and mechanical stability are achieved.

The simplest process for delivering cells involves static seeding, where cells can be delivered onto a

*Author for correspondence (r.m.day@ucl.ac.uk).

Electronic supplementary material is available at http://dx.doi.org/10.1098/rsif.2012.0316 or via http://rsif.royalsocietypublishing.org.

Received 17 April 2012
Accepted 14 May 2012

surface via sedimentation under gravitational force. This process is best suited for flat target surfaces but typically the surface must remain undisturbed in a horizontal plane, making it unsuitable for scaffolds with more complex geometries, such as tubular surfaces, or *in vivo* situations where movement or deviation from the horizontal plane is likely to be encountered.

To overcome these limitations, particularly for tubular constructs used for vascular grafts, several more elaborate seeding techniques have been developed. These include electrostatic seeding [4–6], centrifugal force [7,8], dynamic rotational seeding [2,9,10] and vacuum-assisted techniques [11].

Recently, magnetic force has been used to seed magnetic-particle-tagged cells onto the lumenal surface of tubular scaffolds, using a solenoid-based system, but this approach is limited to small-diameter scaffolds [12]. To overcome this limitation, this study tests the hypothesis that the use of a Halbach cylinder of permanent magnets enables delivery of magnetically tagged cells to the luminal surface of large tubular constructs in a more efficient and uniform manner than a standard, dynamic, rotational cell-seeding approach. To determine this, the performance and reproducibility of a novel, Halbach cylinder cell-seeding device was qualitatively and quantitatively investigated *in vitro* using image analysis and magnetic resonance imaging (MRI) for its ability to deliver superparamagnetic iron oxide nanoparticle (SPION)-tagged cells onto tubular constructs and compared with a dynamic, rotational cell-seeding method.

2. MATERIAL AND METHODS

2.1. Halbach cylinder apparatus

The magnetic seeding device consisted of a bespoke Halbach cylinder (k4 variety; 12 elements with 120° rotation steps for the magnetization orientation; manufactured by Magnet Sales, Swindon, UK; see figure 1 and electronic supplementary material, figure S1). A cylinder (height: 85 mm; diameter: 30 mm) was machined from a solid aluminium block to hold a 50 ml polypropylene conical tube (30 × 115 mm style; Blue MAX Falcon, Becton–Dickinson Labware Europe, Le Pont De Claix, France). Twelve magnetic rods (neodymium–iron–boron magnet NdFeB N48M, remanence magnetization: 1.43 T, intrinsic coercivity: 1120 kA m^{-1}; height: 75 mm; diameter: 8 mm) were equally spaced around the wall of the cylinder. The base of the cylinder contained a cone-shaped battery-powered turntable that was set to rotate at 20 rpm and could be operated externally. The drive motor was contained in a plastic housing allowing the whole device to be placed in a humidified incubator.

2.2. Cell culture

L929 cells derived from C3H/An mouse connective tissue (85011425, Health Protection Agency Culture Collection, Health Protection Agency, Salisbury, UK) were cultured in complete medium consisting of Dulbecco's modified Eagle's medium (MEM) (Sigma-Aldrich, Poole, UK) supplemented with 10 per cent foetal bovine serum (Gibco, Paisley, UK), 2 mM glutamine (Sigma-Aldrich) and 50 U ml^{-1} penicillin and 50 μg ml^{-1} streptomycin (Sigma-Aldrich).

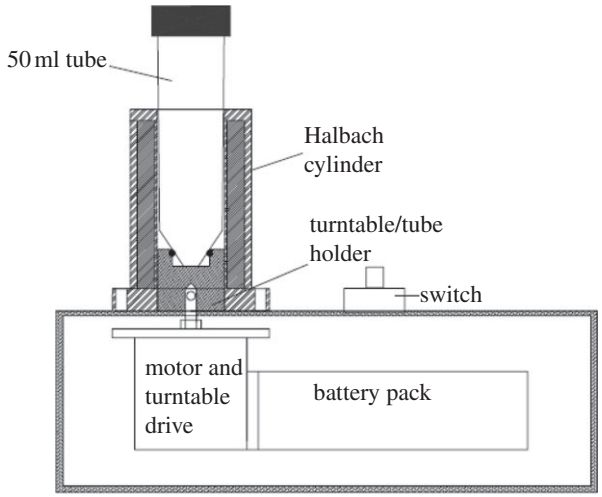

Figure 1. A schematic of the Halbach cylinder cell-seeding device. The Halbach cylinder consisted of 12 NdFeB rods, 75 mm long, with a 120° rotation angle for the magnetization orientation set into aluminium housing. The bore of the cylinder was designed to house a 50 ml tube that holds the membrane scaffolds during the delivery process.

2.3. Loading and quantification of superparamagnetic iron oxide nanoparticle in L929 cells

The SPION (fluidMAG-UC/A; Chemicell GmbH, Berlin, Germany) used for cell loading consisted of an aqueous dispersion with a stock concentration of 40 mg ml^{-1} and a particle density of approximately 1.3×10^{16} particles per gram. The SPION were uncoated and had an anionic surface charge. The particle size, determined by the manufacturer using photon correlation spectroscopy, was 50 nm, which corresponds to the hydrodynamic diameter of the multicore domain structures consisting of a cluster of several 8–15 nm single-domain iron oxide crystals.

L929 cells were grown in 75 cm^2 tissue culture flasks and were incubated at 37°C and 5 per cent CO_2 in complete medium supplemented with SPION at a final concentration of 500, 250, 125, 62.5, 31.25 or 0 μg ml^{-1}. After 24 h incubation, the cells were washed four times with 10 ml of phosphate-buffered saline (PBS) and detached by trypsinization. From each SPION concentration, 1×10^6 cells were lyophilized overnight. The amount of SPION loaded into the cells was measured by superconducting quantum interference device (SQUID) magnetometry. A quantum design SQUID-VSM magnetometer (Quantum Design Inc., San Diego, CA, USA) was used to apply a magnetic field to each sample in the range of 7 T to −7 T. The corresponding magnetic moment and magnetic saturation were measured at a temperature of 300 K. The diamagnetic component was calculated using the linear regions of the graph and subtracted from the magnetic moment. The corrected moment was used to construct closed hysteresis loops, and the SPION mass per cell based upon a saturation

magnetization for the SPION of 73 emu g^{-1} was plotted against the concentration of SPION in the incubation medium.

2.4. Ultrastructural localization of superparamagnetic iron oxide nanoparticles

Transmission electron microscopy (TEM) was used to determine the cellular localization of SPION. After loading and washing, samples were fixed in Karnovsky's fixative and subsequently post-fixed in a solution of phosphate-buffered 1 per cent osmium tetroxide for just 30 min to avoid any contrast masking on the SPION. After a progressive dehydration series in water/acetone mixtures (25%, 50%, 75%, 95%, 100% and 100% over molecular sieves), the cells were resuspended twice in propylene oxide as a transition solvent before the embedment stage. In order to enhance the infiltration of samples with an Araldite CY212 resin (Agar Scientific), two further stages of 90 min each in mixtures of 1 : 3 and 1 : 1 resin/propylene oxide at room temperature were allowed, after which the cells were embedded in pure Araldite medium at 60°C for 36 h. The resulting blocks were thin-sectioned in an ultramicrotome and directly collected on copper grids for its examination under a JEOL JEM 1200EX TEM operating at 80 kV.

2.5. The effect of superparamagnetic iron oxide nanoparticle loading on cytotoxicity and cell viability

L929 cells (1×10^4 cells in 300 µl complete medium) were seeded into 24-well plates (Corning B.V. Life Sciences) and incubated at 37°C in 5 per cent CO_2 for 24 h. The medium was removed and replaced with fresh complete medium containing 500, 250, 125, 62.5, 31.25 or 0 µg ml^{-1} SPION. After 24 h incubation at 37°C in 5 per cent CO_2, the culture medium was removed from the cells and 150 µl from each well was transferred into a 96-well plate. The cells attached to the 24-well plate were washed four times with PBS before replacing with fresh culture medium ready for cell viability assaying or further incubation for a total of 2, 3 and 6 days post-SPION loading.

Release of lactate dehydrogenase (LDH) was used as an indicator of cell cytotoxicity and measured with the Cytotox 96 non-radioactive assay kit (Promega). To separate unbound SPION from the collected supernatant, permanent neodymium magnets (diameter: 14 mm) were placed under the wells of the 96-well plate for 60 min. About 50 µl of the SPION-free supernatant was transferred into fresh wells on a 96-well plate, and the assay was performed according to the manufacturer's instructions.

Cell viability of the SPION-loaded cells attached to the 24-well plate was measured using a CellTiter 96 AQ_{ueous} assay kit (Promega) according to the manufacturer's instructions.

To assess the longer term effect of loading cells with SPION on viability and cytotoxicity, labelled cells were incubated for a total of 2, 3 and 6 days post incubation with SPION and treated as outlined earlier, prior to cytotoxicity and cell titre assays.

2.6. Cell loading using the Halbach cylinder

Nuclepore polycarbonate membranes (Whatman, UK; 25 × 80 mm, 10 µm thick) were rolled and inserted into 50 ml Falcon tubes, resulting in coverage of the lumenal surface of the tube. The membranes were then coated with 10 µg ml^{-1} fibronectin (Sigma-Aldrich).

A 20 ml cell suspension of 1×10^6 L929 cells loaded with SPION after 24 h pre-incubation in medium containing 125 µg ml^{-1} SPION (as outlined earlier) was added to the Falcon tubes containing the polycarbonate membranes. The tubes were placed vertically into the Halbach cylinder and incubated at 37°C for 2 h. Control cells, consisting of 1×10^6 non-SPION-labelled L929 cells, were delivered to the Halbach cylinder in the same manner.

For dynamic, rotational cell seeding, 1×10^6 non-SPION-labelled L929 cells were added to 20 ml of MEM in Falcon tubes containing fibronectin-coated polycarbonate membranes. The tubes were placed horizontally onto a support and incubated at 37°C for 30 min before rotating 90° along the horizontal axis. The rotation process was repeated three times, resulting in a total incubation period of 2 h.

After incubation, the polycarbonate membranes were gently washed once with 30 ml of PBS to remove non-adherent cells and fixed with 2 per cent formaldehyde in 0.1 M PBS (VWR International Ltd, Lutterworth, UK) for 10 min. Fixed membranes were covered with Harris haematoxylin solution (Sigma-Aldrich) for 10 min and washed three times with water. The stained membranes were mounted onto glass slides using aqua-mount aqueous mounting medium (VWR Internation Ltd, Lutterworth, UK). For DAPI images, non-stained membranes were mounted onto glass slides Vectashield Mounting Medium with DAPI (Vector Laboratories Inc., Burlingame, CA, USA).

The number of cells attached to the membranes that underwent dynamic rotational seeding was counted in eight different positions using light microscopy. The positions corresponded with the poles of the four rotated positions and the four positions in between these points of rotation (figure 2). The x–y coordinates from the eight positions on the dynamic rotational membranes were used to define the positions for cell counting on the membranes that underwent cell delivery, using the Halbach array. Cell counts were collected from five replicates for each cell-delivery method.

The rate of cell attachment to the membranes after 30 min incubation (assessed using the Halbach cylinder) was compared with cell attachment to horizontal flat membranes (assessed using a cell-adhesion assay based on a earlier-described method) [13]. Briefly, 5×10^5 cells pre-incubated with medium containing 125 µg ml^{-1} SPION were added to fibronectin-coated membranes in Falcon tubes or to horizontal membranes in a dish with the same dimensions (width and length) as the membrane. The membranes were incubated for 30 min at 37°C in 5 per cent CO_2 before rinsing to remove non-attached cells and fixing in 2 per cent formaldehyde. A control group representing 100 per cent

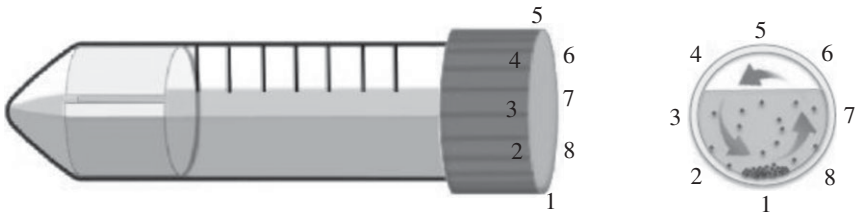

Figure 2. For dynamic, rotational cell seeding, the tubes containing membranes were rotated by 90° counter clockwise after 30 min incubation, resulting in positions 1, 3, 5 and 7 being chronologically located at the 6 o'clock position of the horizontally mounted tube. Positions 2, 4, 6 and 8 were not located at this position during the seeding process.

cell attachment consisted of the same number of cells incubated on the horizontal membranes for 4 h. Cells attached to the membranes were stained with 0.1 per cent crystal violet for 60 min and washed three times with deionized water. The dye was solubilized from the cells by incubating the membranes in 2 ml of 10 per cent acetic acid on an orbital shaker set at 150 rpm for 5 min. One hundred microlitres of supernatant was transferred to a 96-well plate and the absorbance recorded at 570 nm.

2.7. Application of the Halbach cylinder device to gastrointestinal tissue

The feasibility of applying the Halbach cylinder device to the delivery of cells in gastrointestinal tissue was qualitatively evaluated using segments of porcine jejunum obtained from an abattoir. After cutting the specimen into 70 mm lengths, the mesentery was trimmed away and the lumen rinsed several times with PBS before being inverted to expose the mucosa. The mucosal surface was mechanically denuded by scraping with the edge of a glass microscope slide before rinsing with PBS. The jejuna segments were reinverted before being positioned into 50 ml Falcon tubes with stents inserted 1 cm into the ends of each segment so that the lumen remained open. The tubes were filled with 50 ml of complete medium containing a suspension of 1×10^6 L929 cells pre-incubated with medium containing 125 $\mu g\ ml^{-1}$ SPION for 24 h. The tubes were loaded into either the rotating Halbach cylinder and incubated for 2 h at 37°C 5 per cent CO_2 or placed horizontally onto a support and incubated at 37°C for a total of 2 h, with 90° rotation every 30 min, as outlined already. After incubation, the culture medium was removed and the lumen of the jejunum gently washed once with PBS to remove unattached cells, followed by fixation in 2 per cent formaldehyde solution for 24 h.

2.8. Distribution of superparamagnetic iron oxide nanoparticle-loaded cells

MRI was used to qualitatively evaluate the distribution of SPION-loaded cells on the polycarbonate membranes and denuded tissue. The lumen of the tubes containing polycarbonate membranes or denuded jejunum was filled with 1 per cent low melting point agraose (Fermentas Ltd, Hanover MD, USA) containing 8 mM of gadolinium–DTPA (Magnevist, Bayer AG, Berlin, Germany). Imaging was performed on a horizontal bore 9.4 T DirectDrive VNMRS system (Agilent Technologies, Palo Alto CA, USA) using a 35 mm quadrature birdcage volume coil (RAPID Biomedical GmbH, Würzburg, Germany). For three-dimensional imaging, a gradient-echo sequence with the following parameters was used: echo time 6 ms, repetition time 25 ms, flip angle 60°, three averages, field of view $35 \times 29 \times 29$ mm, matrix size $1000 \times 828 \times 828$ leading to an isotropic voxel size of 35 μm. Segmentations and three-dimensional renderings were performed using Amira visualization software (v. 5.2.2, Visage Imaging Inc., Andover MA, USA). Superparamagnetic iron oxide particles cause a perturbation of the magnetic field, which causes enhanced MRI relaxation and leads to local hypointensities in an image [14]. The cross section of the tubes was divided into four segments. For each of these segments, hypo-intense regions indicative of iron content were segmented using thresholds. Volume rendering without smoothing was performed for all segments, and the hypointensity volumes were recorded.

2.9. Statistical analysis

Differences in the distribution of cell attachment between the magnetic and dynamic rotational cell-delivery techniques were analysed as a 2×8 repeated measures experimental design with one between-group factor (the presence or the absence of the Halbach cylinder device) and one within-group factor (the position of cell measurements). A mixed between–within subjects analysis of variance (ANOVA) was conducted to assess the impact of the presence of the Halbach cylinder on cell numbers, across the eight different positions (positions 1–8) [15]. Partial eta-squared (η^2) was calculated to estimate the effect that the size had on significant between-group mean differences [16,17]. Additional comparisons between various positions in each group—according to the presence of the Halbach array—were conducted using a one-way ANOVA. Significance was examined with Tukey's honestly significant difference test for multiple comparisons. SPSS v. 17.0 and GraphPad Prism v. 5.03 were used for all data analyses.

3. RESULTS

3.1. Cell loading with superparamagnetic iron oxide nanoparticles

Cells were incubated in culture medium containing a range of SPION concentrations to evaluate uptake and any effects on cell viability. Cells incubated with SPION for 24 h contained endosomes located in the

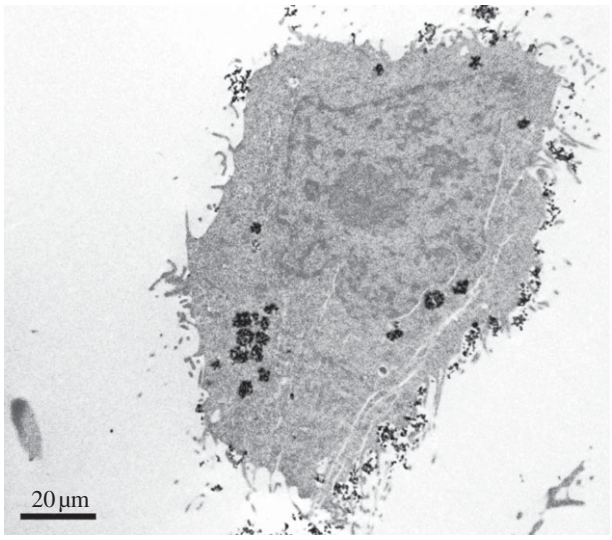

Figure 3. A transmission electron micrograph of an L929 cell pre-incubated with medium containing 125 µg ml^{-1} SPION for 24 h. Endosomes containing SPION are visible as discrete regions within the cytoplasm. Smaller clusters of SPION are also present in pockets created by invaginations of the cell membrane indicating SPION uptake is mediated primarily by endocytosis.

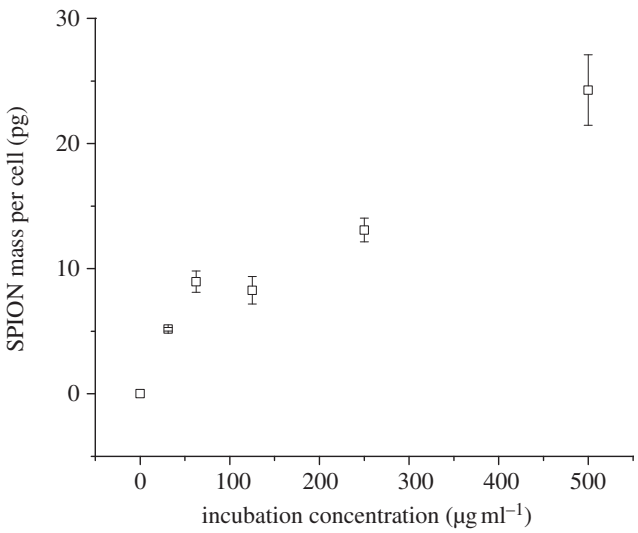

Figure 4. SPION concentration per cell as a function of incubation concentration calculated from SQUID magnetometry.

cytoplasm filled with iron oxide nanoparticles (figure 3). Data from SQUID analyses indicated a direct correlation between the content of SPION in the cells and increasing SPION concentration in the culture medium for the concentrations assessed (figure 4). A 4 µl SPION sample at 40 mg ml^{-1} had a saturation magnetization of 73 emu g^{-1} with an approximate particle magnetization of 5.6×10^{-15} emu per particle. These calculations lead to an average particle concentration of 8.3 pg per cell and approximately 1500 particles per cell for a SPION culture concentration of 125 µg ml^{-1}. Incremental increases in the concentration of SPION from 31.25 to 500 µg ml^{-1} in the culture medium produced no decrease in cell viability, indicated by no significant changes in the release of LDH or reduction in metabolic activity compared with non-loaded control cells (figure 5).

The longer term effects of SPION loading on cell viability after 24 h incubation with 125 µg ml^{-1} SPION was assessed at 1, 2, 3 and 6 days post-loading. SPION loading at this concentration had no negative effect on cell metabolic activity or release of LDH compared with non-loaded control cells. However, a small decrease in LDH release was observed at days 2 and 6 post-loading (figure 5).

3.2. Cell distribution on scaffold membranes

Cell suspensions derived from cultures pre-incubated for 24 h in medium containing 125 µg ml^{-1} SPION were delivered onto polycarbonate membrane scaffolds using the Halbach cylinder device. The distribution of cells was compared with a conventional, dynamic rotational seeding technique. The mean number of cells in each of the eight recorded positions is shown in figure 6. With the Halbach cylinder device, the number of cells at different positions did not significantly differ, whereas the number of cells decreased from position one to position eight in the group seeded using the dynamic rotational seeding technique. The assumption of homogeneity of variance was met because Levene's test of equality of error variance for most positions was non-significant [15]. There was a substantial main effect for the position of measurement (Wilks' $\lambda = 0.007$, $F_{7,2} = 37.86$, $p = 0.026$, partial $\eta^2 = 0.993$), suggesting that there was a change in number of cells over the eight positions. The main effect comparing the two cell-delivery techniques was also significant ($F_{1,8} = 78.97$, $p < 0.0001$, partial $\eta^2 = 0.908$), suggesting that there was a change in number of cells at each position according to the cell-delivery technique. The model had a significant interaction effect between seeding method and position, suggesting that the number of cells in each position was different in each of the two groups (Wilks' $\lambda = 0.005$, $F_{7,2} = 59.74$, $p = 0.017$, partial $\eta^2 = 0.995$), which did not allow interpretation of the main effects of each variable in the combined model independently. Therefore, interpretation of the results took into consideration the estimated marginal mean plot (data not shown) [16,17]. This graph revealed that when cells were seeded with the dynamic rotation method, the cell count decreased from position 1 to 8 in a more obvious manner than when cells were seeded using the Halbach cylinder device, where the number of cells showed a fairly small variation.

To determine the positional effect of the scaffold in each device on the number of cells delivered, a one-way ANOVA was performed for each delivery method (see electronic supplementary material, table S1). For the Halbach cylinder, no significant differences were found in the cell counts between the different positions, whereas in the dynamic rotational seeding group, multiple significant differences were found between various positions (see electronic supplementary material, table S2).

Power of analysis was analysed with G*Power v. 3. On the basis of the sample size of the Halbach cylinder device and dynamic rotation seeding group, post hoc analysis of the power to detect a significant difference (based on $\alpha = 0.05$ with an affect size of 0.908) was approximately 0.99. The average correlation between different position measurements was 0.353, while the non-sphericity correction ε was 0.565 [18,19].

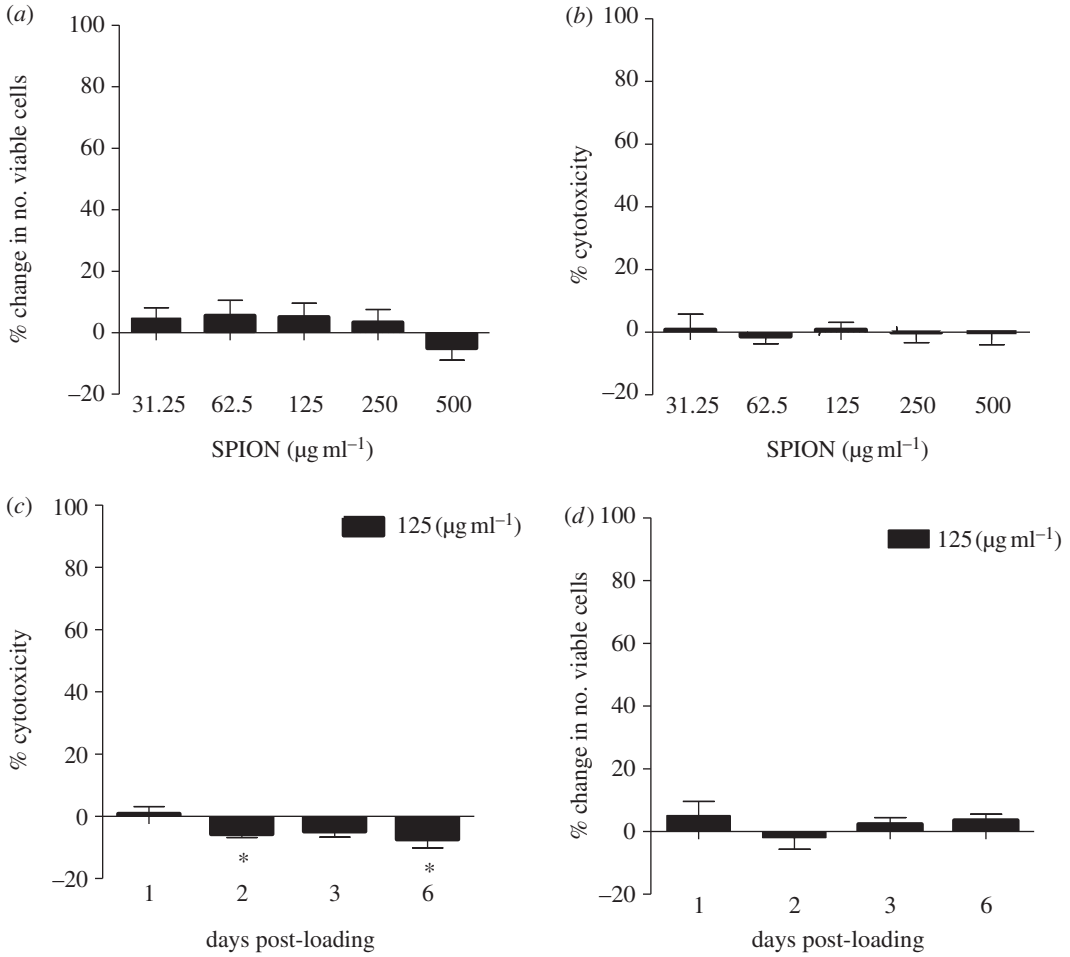

Figure 5. Incubation of L929 cells with SPION resulted in no significant reduction cell viability or increase in cytotoxicity.

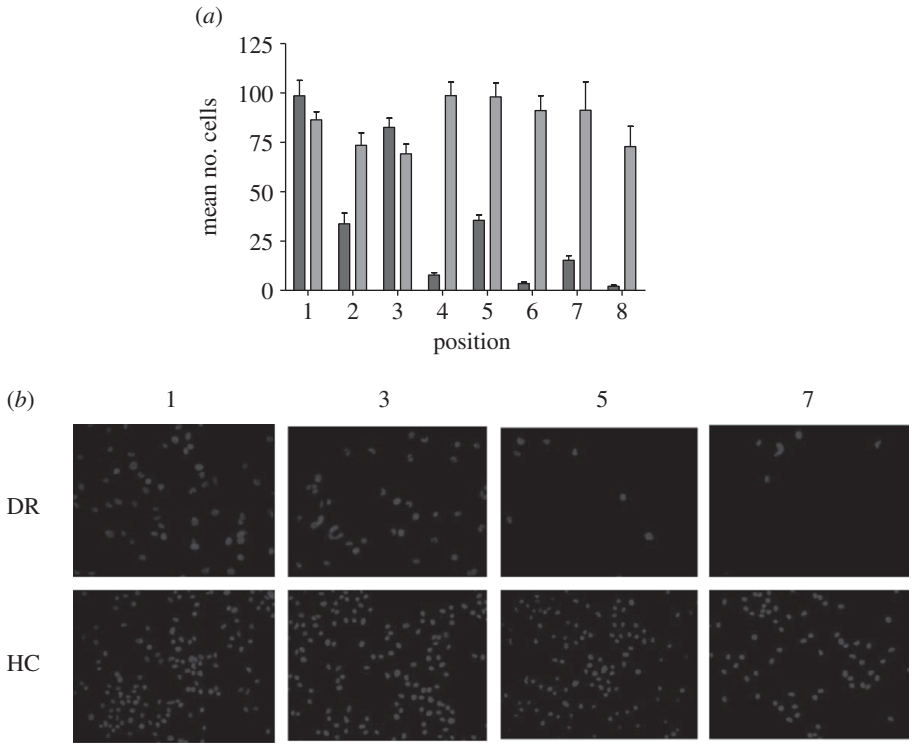

Figure 6. Distribution of L929 cells incubated with 125 μg ml^{-1} SPION after attachment to the polycarbonate membranes. (*a*) The mean number of cells counted at each position on the membrane for cell seeding with dynamic rotation seeding (red colour bars) and Halbach cylinder seeding (blue colour bars). (*b*) The distribution of cells labelled with DAPI attached to the membranes at positions 1, 3, 5 and 7 after seeding with dynamic rotation (DR) or the Halbach cylinder (HC).

Table 1. The percentage of SPION-loaded cells per sector corresponds to the amount of iron-labelled cells in each quadrant with respect to the total amount of iron-labelled cells within that sample.

	percentage of total SPION loaded cells per sector			
	purple	blue	red	green
dynamic rotational seeding	42.7	34.1	14.0	9.1
Halbach cylinder (rotated)	23.9	25.9	25.9	24.7
Halbach cylinder (static)	25.8	23.2	25.0	26.0

MRI confirmed the distribution of SPION-loaded cells on the polycarbonate membranes achieved with each technique. Membranes with cells attached after delivery by dynamic rotational seeding revealed reductions in the amount of SPION-labelled cells delivered in each quadrant corresponding with each subsequent rotation of the membrane (see table 1 and electronic supplementary material, figure S2). The distribution of cells delivered onto membranes rotated in the Halbach cylinder was not significantly different from the distribution of cells delivered in the static, non-rotated Halbach cylinder (see table 1 and electronic supplementary material, figure S2).

3.3. Rate of cell attachment

Cells delivered to membranes using the Halbach cylinder attached more rapidly compared with cells delivered to membranes under gravitational force. After 30 min incubation, significantly more cells were attached to membranes incubated in the Halbach cylinder compared with the number of cells attached after delivery under gravitational force (figure 7).

3.4. Gastrointestinal tissue

The feasibility of applying the Halbach device to the delivery of cells to thick-walled tissue samples was assessed using denuded porcine jejuna. Qualitative assessment of the distribution of cells attached to the tissue by use of MRI revealed a uniform pattern of distribution similar to that observed with the polycarbonate membranes, whereas a non-uniform distribution of cells was observed with the sample loaded by dynamic rotational cell seeding (see electronic supplementary material, figure S2).

4. DISCUSSION

The ability to efficiently load cells onto the luminal surface of tubular scaffolds in a uniform manner is an essential requirement for tissue engineering of hollow organs such as those found in the gastrointestinal tract, airway and vasculature. Recent studies using pre-clinical models have highlighted the need for new techniques to enable rapid and efficient cell delivery onto hollow organ scaffolds.

One example of this is a promising rat model of intestinal tissue engineering. Approximately one-and-a-half

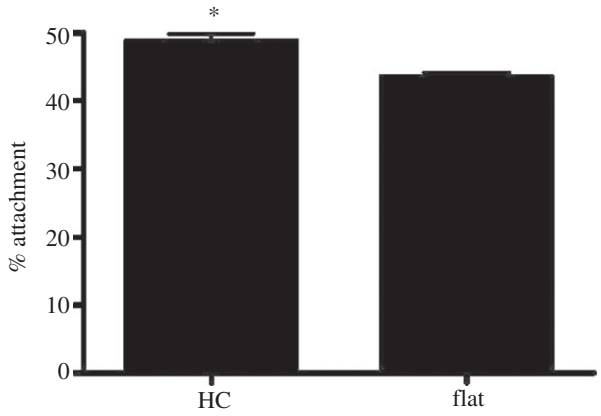

Figure 7. Rate of cell attachment to membranes. After 30 min incubation significantly more cells were attached to membranes delivered using the Halbach cylinder (HC) compared with cells delivered onto flat membranes under gravitational force ($*p < 0.05$). Figures shown represent the percentage of cells attached to the membranes after 30 $\mu g\,ml^{-1}$ min incubation compared with control flat membranes.

donor intestines are needed to seed a construct that is only 10 mm in length and has a luminal diameter of 2–4 mm [20]. This represents a 2 per cent seeding efficiency on the basis of the amount of neointestine formed from the harvested native intestine. Much larger scaffolds are often necessary if pre-clinical technology such as this is to be translated into a human application. In this case, the normal non-distended luminal diameter of the small intestine in adult humans is approximately 30 mm [21]. Similarly, *in vivo* cell transplantation of oesophageal epithelial cells into a devitalized rat trachea, implanted under the dorsal skin of mice, resulted in a stratified epithelium, but the optimal time to regenerate confluent epithelium was six weeks [22]. The uneven distribution of cells observed after three weeks is likely to have contributed to the delay in achieving confluency [22].

To overcome the limitations of conventional seeding techniques, a variety of alternative methods have been devised. While most of these approaches offer improved seeding efficiencies compared with static seeding methods, most have been used only for small-scale constructs and offer little promise for large tubular organs. Dynamic rotational seeding, where a scaffold is rotated along its longitudinal axis to distribute cells over the surface of the scaffold lumen, has been used to seed autologous cells onto the lumen of decellularized trachea, prior to transplantation into a human recipient [2]. Although the study was clinically successful, it is not clear how many of the cells delivered attached to the scaffold or whether there was uniform distribution of cells. The prolonged and continuous movement between the cell suspension and scaffold surface over a period of 96 h indicates that this approach provided suboptimal conditions for promoting cell attachment to the scaffold. Furthermore, dynamic seeding can expose cells to undesired wall shear stress, causing phenotypic changes to the cells [9].

Magnetic field gradients have previously been used to deliver cells onto the lumenal surface of small tubular scaffolds. A solenoid-based approach described by Perea *et al.* [12] required the scaffold to be placed above the upper extreme of the solenoid coil where the radial

magnetic field gradient existed. The radial magnetic force generated rapidly immobilized SPION-tagged cells onto the scaffold surface, allowing cell adhesion to quickly occur (approx. 20 min). However, the solenoid-based approach has limited potential in clinical applications because it is designed primarily for applying to vascular grafts *ex vivo* with relatively small (3–5 mm) lumenal diameters. Furthermore, the area exposed to the optimal magnetic field for cell seeding existed only at the upper extreme of the solenoid, limiting the length of constructs that can be effectively seeded. To achieve a magnetic field with this technique, which is capable of seeding constructs with larger lumenal diameters, such as the small intestine (approx. 20–30 mm diameter), would require a much larger solenoid, which would generate excessive amounts of heat, causing damage to the cells and scaffold if inadequate cooling was provided.

Permanent magnets offer scalable high field strength without the detrimental heating effects associated with solenoid-induced magnetic fields. We have previously magnetically tagged cells with SPION and targeted them to a localized site of arterial injury using a magnetic actuator consisting of a rectangular Halbach array positioned outside the body [23].

This study advances the concept of using permanent magnets to deliver cells into hollow organs via the use of a Halbach cylinder.

L929 cells were used as a surrogate cell type in this study because of its wide use in ISO10993 set of standards for evaluating biocompatibility of medical devices. Incubation of cells in medium containing high concentrations of SPION did not result in an increase in cytotoxicity or in reduced cell metabolism for any of the concentrations tested in this study. The selected concentration of SPION in the culture medium (125 $\mu g\ ml^{-1}$) used for evaluating the Halbach device was not the highest concentration tested but provided sufficient cell uptake for magnetic actuation to occur. This concentration caused a slight reduction in the amount of LDH release from cells measured between 2 and 6 days after incubation with SPION compared with control cells. These data, taken together with the data showing no change in cell viability at the same time points, indicate that 125 $\mu g\ ml^{-1}$ SPION used for cell loading was not cytotoxic. The mechanism causing the reduction of LDH release from SPION-loaded cells is unaccounted for but might be related to SPION improving retention of membrane integrity over the time period studied. Although data (not shown) from our group and elsewhere indicate that similar SPION uptake into endosomes in the cytoplasm occurs with other cell types, including smooth muscle and epithelium that are relevant to gastrointestinal tissue engineering, it is likely that SPION concentration in the culture medium would need to be optimized for each type of cell receiving magnetic actuation.

SPION-labelled cells delivered into the lumen of tubular membrane scaffolds or segments of porcine jejuna positioned inside the Halbach cylinder were exposed to an intense magnetic field and drawn to the surface of the scaffold. The majority of SPION-labelled cells were attached to the membrane within the 2 h incubation used in this study as a comparison with the previously reported dynamic rotation technique used for seeding cells onto decellularized trachea prior to the clinical transplantation. The increased rate of cell attachment observed with Halbach cylinder delivery process therefore suggests that the amount of time needed for cell delivery could be reduced to less than 2 h.

Cells delivered onto the membrane scaffolds and porcine jejuna, using the dynamic rotation technique, were unevenly distributed, with fewer cells attached at consecutive points of rotation. The Halbach cylinder device resulted in a uniform distribution of cells attached that did not vary significantly between the reference points on the membranes selected from the dynamic rotation samples. The capacity to rotate the scaffold inside the Halbach cylinder, designed to overcome the possibility of cells being aligned in vertical bands corresponding to the positions of the 12 magnetic elements, was found to be unnecessary because there was no significant difference in cell distribution between the rotated and non-rotated Halbach cylinder membranes.

The ability to deliver cells with uniform distribution onto tubular scaffolds holds great value for the engineering of hollow organs. Previous studies have demonstrated that the extent of circumferential coverage of the oesophagus after endoscopic mucosal resection is indirectly correlated with the likelihood of stenosis and stricture formation [24]. It is possible that the non-uniform distribution of cells onto tubular scaffolds, observed with the dynamic rotation seeding method in this study, might increase the risk of subsequent stricturing of the construct caused by unequal distribution of tissue in the construct. The even distribution of cells achieved with the Halbach cylinder device is likely to reduce the risk of this occurrence.

This study demonstrates proof-of-principle that a Halbach device was capable of delivering SPION-loaded cells onto the lumenal surface of isolated segments of jejuna whose walls were considerably thicker (1–2 mm) compared with the polycarbonate membranes. On the basis of these rudimentary findings, it is feasible that a similar compact permanent magnet device could assist with surgical techniques where the delivery of cell suspensions or sheets of cells to the luminal surface of hollow organs is required, which would be difficult to achieve with electromagnets. This might include *in situ* delivery and engraftment of adult stem cells in therapeutic applications for patients with enteropathies associated with dysfunctional intestinal epithelium (microvillus inclusion disease), mucositis (chemo- or radiation therapy induced), intestinal graft versus host disease or short bowel syndrome. This process could be aided *in situ* by using a Halbach cylinder that is hinged or clamped so that it could be positioned around a segment of continuous bowel. Furthermore, the use of the Halbach cylinder for cell delivery offers the possibility of delivering consecutive layers of different cell types to laminated tissues with distinct functional layers, such as those found in the gastrointestinal and airway tracts. A positive side effect of magnetic cell delivery is the ability to use non-invasive clinical or preclinical MRI to assess the success and quality of cell engraftment prior to the implantation of a scaffold or *in vivo* for *in situ* delivery strategies [25–27]. Optimization of the configuration of magnets for specific tissues will enable the seeding method to be tailored for tissues of

different shapes and sizes, as well as defined bands of tissue, such as cartilage found in the larynx and trachea.

5. CONCLUSION

The novel concept of a Halbach cylinder for tissue engineering provides an adaptable and efficient solution for delivering cells in a rapid and uniform manner for therapeutic applications.

The authors are grateful for the support of the Crucible Centre UCL and the British Heart Foundation. This work was undertaken at UCL/UCLH, which receives funding from the Department of Health's NIHR as a Comprehensive Biomedical Research Centre.

REFERENCES

1 Shin'oka, T., Imai, Y. & Ikada, Y. 2001 Transplantation of a tissue-engineered pulmonary artery. *N. Engl. J. Med.* **344**, 532–533. (doi:10.1056/NEJM200102153440717)
2 Macchiarini, P. *et al.* 2008 Clinical transplantation of a tissue-engineered airway. *Lancet* **372**, 2023–2030. (doi:10.1016/S0140-6736(08)61598-6)
3 Atala, A., Bauer, S. B., Soker, S., Yoo, J. J. & Retik, A. B. 2006 Tissue-engineered autologous bladders for patients needing cystoplasty. *Lancet* **367**, 1241–1246. (doi:10.1016/S0140-6736(06)68438-9)
4 Bowlin, G. L., Meyer, A., Fields, C., Cassano, A., Makhoul, R. G., Allen, C. & Rittgers, S. E. 2001 The persistence of electrostatically seeded endothelial cells lining a small diameter expanded polytetrafluoroethylene vascular graft. *J. Biomater. Appl.* **16**, 157–173. (doi:10.1106/NCQT-JFV9-2EQ1-EBGU)
5 Fields, C., Cassano, A., Allen, C., Meyer, A., Pawlowski, K. J., Bowlin, G. L., Rittgers, S. E. & Szycher, M. 2002 Endothelial cell seeding of a 4-mm I.D. polyurethane vascular graft. *J. Biomater. Appl.* **17**, 45–70. (doi:10.1177/088532820201700186)
6 Fields, C., Cassano, A., Makhoul, R. G., Allen, C., Sims, R., Bulgrin, J., Meyer, A., Bowlin, G. L. & Rittgers, S. E. 2002 Evaluation of electrostatically endothelial cell seeded expanded polytetrafluoroethylene grafts in a canine femoral artery model. *J. Biomater. Appl.* **17**, 135–152. (doi:10.1106/088532802030556)
7 Godbey, W. T., Hindy, S. B., Sherman, M. E. & Atala, A. 2004 A novel use of centrifugal force for cell seeding into porous scaffolds. *Biomaterials* **25**, 2799–2805. (doi:10.1016/j.biomaterials.2003.09.056)
8 Soletti, L., Nieponice, A., Guan, J., Stankus, J. J., Wagner, W. R. & Vorp, D. A. 2006 A seeding device for tissue engineered tubular structures. *Biomaterials* **27**, 4863–4870. (doi:10.1016/j.biomaterials.2006.04.042)
9 Hsu, S. H., Tsai, I. J., Lin, D. J. & Chen, D. C. 2005 The effect of dynamic culture conditions on endothelial cell seeding and retention on small diameter polyurethane vascular grafts. *Med. Eng. Phys.* **27**, 267–272. (doi:10.1016/j.medengphy.2004.10.008)
10 Nasseri, B. A. *et al.* 2003 Dynamic rotational seeding and cell culture system for vascular tube formation. *Tissue Eng.* **9**, 291–299. (doi:10.1089/107632703764664756)
11 Nieponice, A., Soletti, L., Guan, J., Deasy, B. M., Huard, J., Wagner, W. R. & Vorp, D. A. 2008 Development of a tissue-engineered vascular graft combining a biodegradable scaffold, muscle-derived stem cells and a rotational vacuum seeding technique. *Biomaterials* **29**, 825–833. (doi:10.1016/j.biomaterials.2007.10.044)
12 Perea, H., Aigner, J., Hopfner, U. & Wintermantel, E. 2006 Direct magnetic tubular cell seeding: A novel approach for vascular tissue engineering. *Cells Tissues Organs* **183**, 156–165. (doi:10.1159/000095989)
13 Humphries, M. J. 2001 Cell-substrate adhesion assays *Curr. Protoc. Cell Biol.* 9.1.1–9.1.11. (doi:10.1002/0471143030.cb0901500)
14 Riegler, J., Wells, J. A., Kyrtatos, P. G., Price, A. P., Pankhurst, Q. A. & Lythgoe, M. F. 2010 Targeted magnetic delivery and tracking of cells using a magnetic resonance imaging system. *Biomaterials* **31**, 5366–5371. (doi:10.1016/j.biomaterials.2010.03.032)
15 Tabachnick, B. G. & Fidell, L. S. 2001 *Computer-assisted research design and analysis*, p. 321. Boston, MA: Allyn and Bacon.
16 Pallant, J. 2007 *SPSS survival manual*. Berkshire, UK: Open University Press.
17 Kinnear, P. R. & Gray, C. D. 2010 *PASW Statistics 17 Made Simple*. New York, NY: Psychology Press.
18 Faul, F., Erdfelder, E., Lang, A. G. & Buchner, A. 2007 G*Power 3: a flexible statistical power analysis program for the social, behavioral, and biomedical sciences. *Behav. Res. Methods* **39**, 175–191. (doi:10.3758/BF03193146)
19 Carrion, V. G., Weems, C. F., Ray, R. D., Glaser, B., Hessl, D. & Reiss, A. L. 2002 Diurnal salivary cortisol in pediatric posttraumatic stress disorder. *Biol. Psychiatry* **51**, 575–582. (doi:10.1016/S0006-3223(01)01310-5)
20 Tavakkolizadeh, A., Berger, U. V., Stephen, A. E., Kim, B. S., Mooney, D., Hediger, M. A., Ashley, S. W., Vacanti, J. P. & Whang, E. E. 2003 Tissue-engineered neomucosa: morphology, enterocyte dynamics, and SGLT1 expression topography. *Transplantation* **75**, 181–185. (doi:10.1097/01.TP.0000044101.03656.9F)
21 Herlinger, H. 1999 Anatomy of the small intestine. In *Clinical imaging of the small intestine* (eds D. D. T. Maglinte, H. Herlinger & B. A. Birnbaum), pp. 5–6. New York, NY: Springer.
22 Croagh, D., Cheng, S., Tikoo, A., Nandurkar, S., Thomas, R. J., Kaur, P. & Phillips, W. A. 2008 Reconstitution of stratified murine and human oesophageal epithelia in an *in vivo* transplant culture system. *Scand. J. Gastroenterol.* **43**, 1158–1168. (doi:10.1080/00365520802102489)
23 Kyrtatos, P. G., Lehtolainen, P., Junemann-Ramirez, M., Garcia-Prieto, A., Price, A. N., Martin, J. F., Gadian, D. G., Pankhurst, Q. A. & Lythgoe, M. F. 2009 Magnetic tagging increases delivery of circulating progenitors in vascular injury. *JACC Cardiovasc. Interv.* **2**, 794–802. (doi:10.1016/j.jcin.2009.05.014)
24 Katada, C., Muto, M., Manabe, T., Boku, N., Ohtsu, A. & Yoshida, S. 2003 Esophageal stenosis after endoscopic mucosal resection of superficial esophageal lesions. *Gastrointest. Endosc.* **57**, 165–169. (doi:10.1067/mge.2003.73)
25 de Vries, I. J. *et al.* 2005 Magnetic resonance tracking of dendritic cells in melanoma patients for monitoring of cellular therapy. *Nat. Biotechnol.* **23**, 1407–1413. (doi:10.1038/nbt1154)
26 Nahrendorf, M., Jaffer, F. A., Kelly, K. A., Sosnovik, D. E., Aikawa, E., Libby, P. & Weissleder, R. 2006 Noninvasive vascular cell adhesion molecule-1 imaging identifies inflammatory activation of cells in atherosclerosis. *Circulation* **114**, 1504–1511. (doi:10.1161/CIRCULATIONAHA.106.646380)
27 Panizzo, R. A., Kyrtatos, P. G., Price, A. N., Gadian, D. G., Ferretti, P. & Lythgoe, M. F. 2009 *In vivo* magnetic resonance imaging of endogenous neuroblasts labelled with a ferumoxide-polycation complex. *Neuroimage* **44**, 1239–1246. (doi:10.1016/j.neuroimage.2008.10.062)